The Formic Acid−Trifluoroacetic Acid Bimolecule. Gas-Phase Infrared Spectrum and Computational Studies

John W. Keller[†]

Department of Chemistry and Biochemistry, University of Alaska Fairbanks, Fairbanks, Alaska 99775-6160

Received: January 9, 2004

The gas-phase FT-IR spectrum of the formic acid−trifluoroacetic acid (FA−Tfa) hydrogen-bonded complex, or bimolecule, was obtained by numerical analysis of the FT-IR spectrum of a mixture of FA and Tfa vapors. Nineteen out of 24 vibrational modes predicted by ab initio frequency calculations to occur in the mid-IR range (400−4000 cm^{-1}) were observed as well-defined absorbance peaks, with the other five occurring as complex or overlapped regions. Several hydrogen-bond-influenced vibrations of each monomer were identified, including C═O stretching and COH in-plane and OH out-of-plane bending. These occurred at 1701, 1403, and 871 cm^{-1}, respectively, for FA, and at 1774, 1325, and 942 cm^{-1}, respectively, for Tfa. The hydrogen bond donated by Tfa in the bimolecule appears to be stronger than that in the Tfa dimer, while the FA-donated hydrogen bond is weaker than that in the FA dimer. Geometry optimization and vibrational frequency calculations were carried out at 21 levels of theory up to B3LYP/aug-cc-PVDZ. All levels of theory predicted an unsymmetrical complex, with hydrogen bond distances of 1.608 Å and 1.706 Å donated by Tfa and FA, respectively, and the corresponding O···O distances of 2.620 Å and 2.704 Å (B3LYP/aug-cc-PVDZ). These values differ from the symmetrical, or nearly symmetrical, structure derived from microwave spectra (Costain and Srivastava, *J. Chem. Phys.* **1964**, *41*, 1620−1627; Martinache et al. *Chem. Phys.* **1990**, *148*, 129−140). In agreement with previous experimental findings, the bimolecule was predicted to be more stable than either homodimer, with a calculated $\Delta H_{complexation}$ of −14.2 kcal/mol (B3LYP/aug-cc-PVDZ). Mulliken population analysis predicted a polar complex with a transfer of 0.02−0.03 protons from Tfa to FA and a predicted dipole moment of 2.3−2.4 D, depending on the level of theory. The combined spectroscopic and computational evidence indicates that in this complex the Tfa-donated hydrogen bond is strengthened more than the FA-donated hydrogen bond is weakened.

Introduction

Carboxylic acid dimers serve as models for biological hydrogen-bonded systems such as Watson−Crick base pairs in DNA. They are attractive subjects for physical studies because the low molecular weight dimers can be prepared in the gas phase or in inert gas matrixes where the properties of the hydrogen bonds can be studied directly, without interference from solvation or crystal lattice effects. Carboxylic acid dimers have been scrutinized by many different methods, beginning with a gas-phase electron diffraction study of formic acid (FA) dimer by Pauling and Brockway in 1934.[1] Other approaches have included infrared spectroscopy,[2−8] high-resolution vibrational−rotational spectroscopy,[9] Raman spectroscopy,[2,10−12] gas-phase NMR,[13,14] cavity ring-down spectroscopy,[15] and other physical methods,[16−19] and theoretical studies using semiempirical[20,21] and ab initio[22−25] methods, and density functional theory.[25−28] These studies have shown that the hydrogen bonds of the dimer each contribute about −7 kcal/mol to the enthalpy of interaction, that donor O−H and acceptor C═O bonds are weakened by hydrogen bond formation, and that tunneling provides an important route for H exchange in the complex.[9,14,29]

The symmetry of the carboxylic acid dimer limits in certain ways its relevance as a model for biological systems: cyclic hydrogen-bonded arrays in biological systems usually are unsymmetrical, containing hydrogen bonds of unequal strength with an inherently polar electronic structure. From this point of view, unsymmetrical carboxylic acid complexes containing two different carboxylic acids, which are termed bimolecules,[29] may prove useful especially regarding the nature of the bonding involved when net proton transfer occurs within the complex. The main experimental approach in the study of bimolecules in the gas phase has been microwave spectroscopy,[29−32] in which the polar bimolecule is selectively detected in the presence of monomers and the nonpolar symmetric dimers. Although to date no mid-IR spectrum has been reported for a carboxylic acid bimolecule, these complexes have previously been studied by far-IR spectroscopy,[33,34] vapor density methods,[35] and by thermodynamic analysis of liquid[36] and solid mixtures.[37] The structure of the acetic acid−trifluoroacetic acid (Tfa) bimolecule, which crystallizes from the mixed acids at low temperatures, has been determined.[38]

Theoretical studies of carboxylic acid bimolecules have been limited to semiempirical calculations of complexation energy and overall geometry of the FA−Tfa[21] and acetic acid−Tfa[39] bimolecules. No ab initio or DFT calculations have been reported for carboxylic acid bimolecules.

The first spectroscopic studies of carboxylic acid bimolecules assumed a symmetrical structure as in **1** (Chart 1).[21,29] Later, Martinache et al. investigated the microwave spectra of FA−Tfa using isotopically substituted FA.[32] They were only able to obtain slightly different values for the two O···O distances, due to the difficult interpretation of low-amplitude vibrations, and

[†] E-mail: ffjwk@uaf.edu.

10.1021/jp049883x CCC: $27.50
Published on Web 05/01/2004

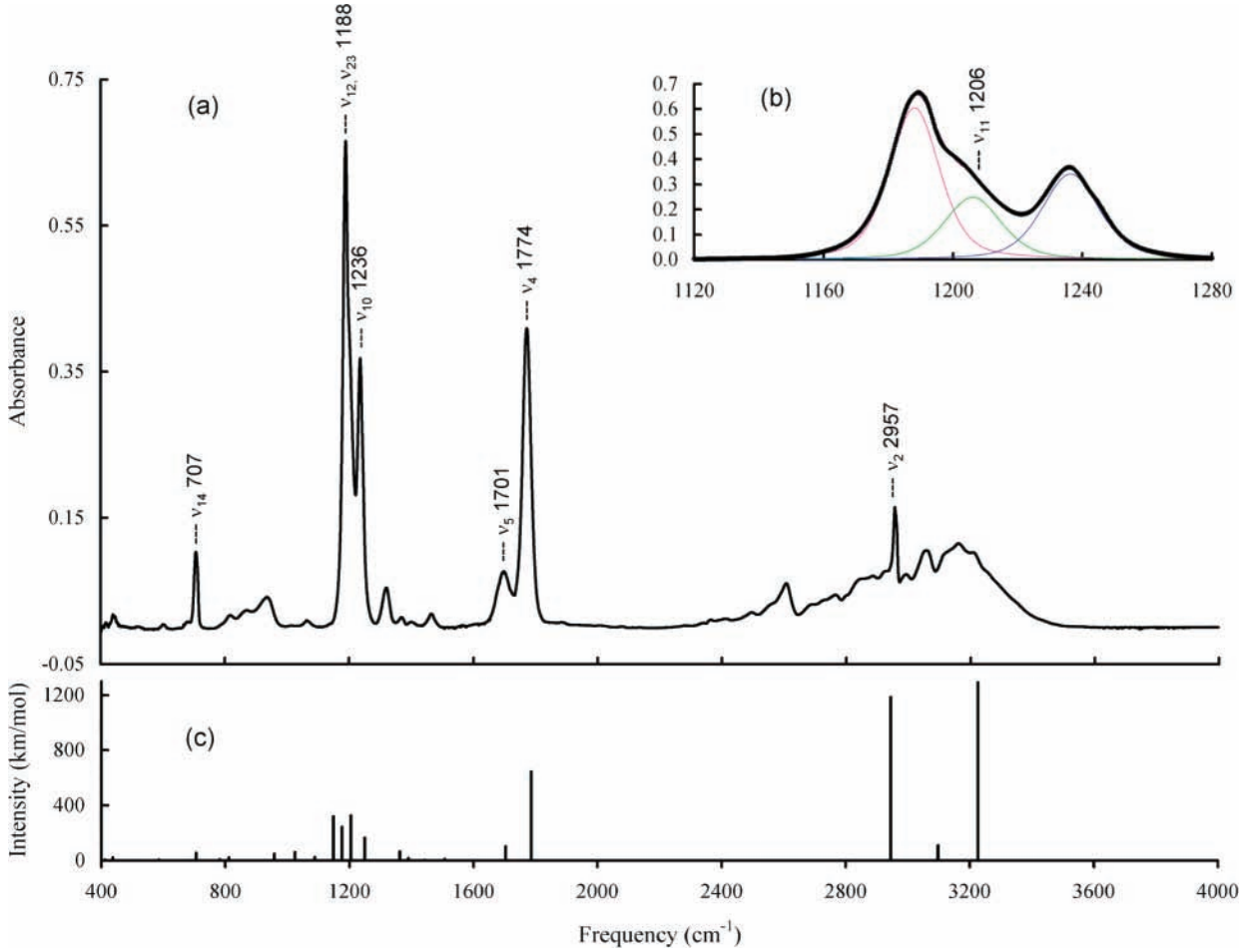

Figure 1. Gas-phase FT-IR spectrum of the formic acid−trifluoroacetic acid bimolecule. (a) Experimental spectrum. (b) Least squares fit of three Lorentzian−Gaussian curves to the 1120−1280 cm^{-1} region of the experimental spectrum. Points are experimental, lines are fitted. (c) Theoretical spectrum (unscaled) calculated at the B3LYP/aug-cc-pVDZ level of theory. Low-intensity peaks are labeled in Figure 2.

CHART 1: Symmetrical (1) and Unsymmetrical (2) Models for Hydrogen Bonding in the Formic Acid−Trifluoroacetic Acid Bimolecule[a]

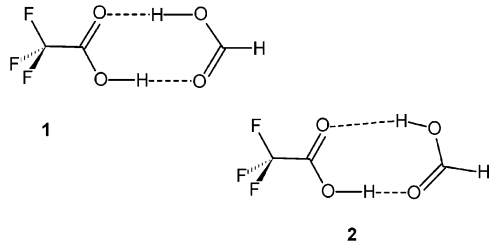

1

2

[a] The FT-IR spectrum and ab initio and DFT calculations indicate that the structure is similar to **2**, although the actual H···O distance differences are smaller than illustrated.

perhaps also because it was assumed that the two O−H bond distances were equal. One might argue that the two hydrogen bonds in the FA−Tfa bimolecule should be similar, considering the similar stabilities and hydrogen bond geometries of the respective dimers[40] and the nearly identical O−H bond distances of FA and Tfa monomers. On the other hand, Tfa is a stronger acid than FA by 3 pK_a units, which could result in a stronger attraction of the Tfa−OH to the FA carbonyl, as in the unsymmetrical structure **2** (Chart 1). In the crystal environment, the acetic acid−Tfa bimolecule does have such an unsymmetrical structure.[38] In this report, gas-phase spectroscopic and computational data are presented that demonstrate unequal proton donation along the hydrogen bonds, resulting in a highly polar and unsymmetrical complex.

Results and Discussion

Infrared Spectrum. The gas-phase mid-IR spectrum of the FA−Tfa bimolecule is shown in Figures 1 and 2. The spectrum was derived from the 0.5-cm^{-1} resolution gas-phase FT-IR spectrum of a mixture of the two acids by subtracting scaled spectra of FA, FA dimer, Tfa, and Tfa dimer. Monomer and dimer spectra were obtained from gas-phase spectra of the separate acids taken at two different total concentrations, using the fact that as the total pressure increases, the dimer concentration increase is proportional to the square of the increase in the monomer concentration.[6] Scale factors for the four known components were manually adjusted to cancel out local spectral features unique to each of the known species. Because of the favorable equilibrium constant for formation of the bimolecule, the residual spectrum comprised a substantial part of the total spectrum: in the spectrum shown in Figure 1, the bimolecule accounted for 50.6% of the total absorbance intensity. The absorbance peaks in the residual spectrum were unchanged with respect to shape, position, and relative intensity in samples containing various amounts of FA and Tfa. Also, 19 peaks in the residual spectrum had close counterparts in the theoretical vibrational spectrum of the FA−Tfa bimolecule. Except for the complex OH stretch region, all peaks in the residual spectrum could be accounted for in the theoretical spectrum. On the basis of these observations, the residual absorbance spectrum (Figures 1 and 2) was assigned to the FA−Tfa bimolecule.

Theoretical Frequency Analysis. The 33 normal modes of the FA−Tfa bimolecule, which are all infrared active due to

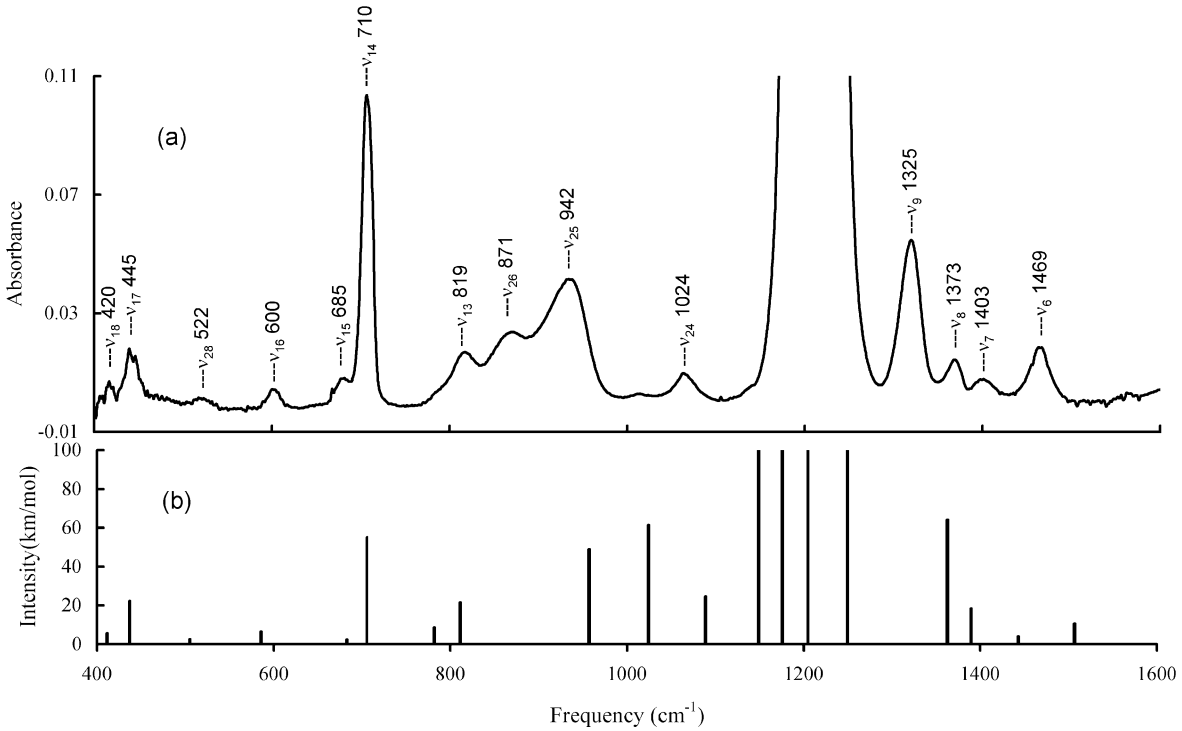

Figure 2. Low-intensity infrared peaks of the formic acid−trifluoroacetic acid bimolecule. (a) Experimental spectrum. (b) The 0−100 km/mol region of the theoretical spectrum calculated at the B3LYP/aug-cc-pVDZ level of theory.

the low symmetry of the complex, are comprised of six intermolecular and 27 intramolecular modes. The intermolecular modes arise from applying the 3N − 6 rule to the complex and subtracting the number of modes expected for the separate monomers. All the intermolecular modes and three Tfa modes (CF_3 rotation, O out-of-plane rotations, and CO_2H in-plane rock) are predicted to occur in the far-IR, leaving 24 to be accounted for in the 400−4000 cm^{-1} region of the spectrum that was accessible in this experiment. The harmonic frequencies of the optimized bimolecule were computed using 20 model chemistries including RHF, MP2, BLYP, and B3LYP methods and basis sets ranging in size from 6-31G (96 basis functions) to aug-cc-pVDZ (257 basis functions). The B3LYP/aug-cc-pVDZ model chemistry provided the best fit between observed and calculated frequencies. Unscaled theoretical frequencies and intensities are plotted in Figures 1c and 2b and are listed in Table 1 along with normal mode assignments. Assignments of the nonoverlapping experimental peaks to the normal modes was based on the calculated order of normal modes, with one exception as noted below. Unscaled calculated frequencies averaged 101.1% of the experimental frequencies, ranging from 96.8% for ν_{23}, the CF_2 out-of-plane stretch, to 110.0% for ν_{26}, the FA OH out-of-plane bend. Relative calculated intensities agreed well enough with the observed spectrum to provide obvious visual alignments of most of the experimental and calculated peaks (Figure 2).

One predicted vibration, ν_{11}, the FA C−O stretching mode, appeared as a shoulder at 1205 cm^{-1}. This peak was located by fitting three Lorentzian−Gaussian functions to the 1120−1280 cm^{-1} region of the experimental spectrum (Figure 1b). The second peak in this region was ν_{10}, the in-plane C−F stretch at 1236 cm^{-1}. The assignments of ν_{10} and ν_{11} were reversed in the B3LYP/aug-cc-pVDZ frequency analysis; however, most of the other DFT and MP2 calculations put the C−O stretch at a lower frequency than that of C−F. Additionally, (i) the intensity of the C−O stretch peak was consistently predicted by various theoretical analyses to be 40−70% of the intensity of the C−F stretch, and in the fitted spectrum ν_{11} is 72% of ν_{10}, and (ii) the frequency shifts of these vibrations going from the respective dimers to the FA−Tfa bimolecule were accurately predicted by most of the higher level frequency analyses. The curve fitting procedure also identified a large peak at 1188 cm^{-1} (Figure 1b). This is due to the near-coincidence of two rather intense peaks whose predicted frequencies are within 27 wavenumbers of each other: ν_{12}, a symmetric CF_3 deformation-C−O stretch combination, and ν_{23}, the out-of-plane CF_2 stretch. Finally, ν_{27}, a low-intensity out-of-plane Tfa carbonyl mode predicted at 782 cm^{-1}, could not be identified in the experimental spectrum. This low-intensity peak probably overlaps ν_{13} near 811 cm^{-1}. A major feature of the FA−Tfa bimolecule FT-IR spectrum is the intense O−H absorbance from 2400 to 3400 cm^{-1}, which is similar in appearance to the spectra of other carboxylic acid dimers. The only identifiable peak in this region is the FA C−H stretch at 2957 cm^{-1}, which is similar in position and shape to those of the FA dimer and monomer.

Comparing H-Bond-Related Vibrations in the Bimolecule, Monomers, and Dimers. The high-frequency O−H stretching vibrations of the bimolecule are obscured in this spectrum, however, other vibrational modes that are diagnostic of the hydrogen bond status within the complex can be identified. These are the oop δCOH bending (ν_{24} and ν_{25}), ip HOC bending (ν_7 and ν_9), and carbonyl stretches (ν_4 and ν_5). The analogous peaks in the known IR and Raman spectra of FA and Tfa monomers and dimers are compared in Table 2.

Out-of-plane δCOH bending vibrations are sensitive to the presence of hydrogen-bonding interactions. In the Tfa dimer, this band is 331 cm^{-1} higher than the analogous band in the spectrum of Tfa monomer, due to the encumbrance of the OH in the cyclic hydrogen bond. The Tfa oop δCOH band in the bimolecule (ν_{25}) is 34 cm^{-1} higher than the corresponding vibration of A_u symmetry in the Tfa dimer. These are compared because in both oop δCOH vibrations the H atoms move up and down together. The higher frequency vibration indicates that in the bimolecule the Tfa OH is encumbered by a stronger

TABLE 1: Vibrational Frequencies (cm^{-1}) and IR Intensities for the Formic Acid−Trifluoroacetic Acid Bimolecule

				frequency		intensity	
		assignment	origin	exptl	(calcd)[a]	exptl[b]	(calcd, km/mol)
A′	1	O−H	FA	*c*	(3225)	s	(1747)
	2	C−H	FA	2957	(3097)	m	(110)
	3	O−H	Tfa	*c*	(2943)	s	(1186)
	4	C═O	Tfa	1774	(1787)	s	(647)
	5	C═O	FA	1701	(1705)	m	(104)
	6	C−O	Tfa	1469	(1507)	w	(11)
	7	HOC	FA	1403	(1444)	w	(4)
	8	HCO	FA	1373	(1390)	w	(18)
	9	HOC	Tfa	1325	(1363)	m	(64)
	10	C−F	Tfa	1236	(1205)	s	(326)
	11	C−O	FA	1206	(1250)	s	(166)
	12	CF_3	Tfa	1188[d]	(1177)	s	(243)
	13	O−C═O	Tfa	819	(811)	w	(22)
	14	O−C═O	Tfa	710	(707)	m	(55)
	15	O−C═O	FA	685	(683)	w	(2)
	16	CO_2H rock	Tfa	600	(586)	w	(7)
	17	δCF_2	Tfa	445	(437)	w	(22)
	18	C−C	Tfa	420	(412)	w	(6)
	19	CO_2H rock ip	Tfa		(299)		(43)
	20	O−H···O ip	inter	200[e]	(218)	w[e]	(10)
	21	O···O	inter	146[f]	(158)		(2)
	22	O−H···O ip	inter	112[e]	(120)	w[e]	(3)
A"	23	CF_2	Tfa	1188[d]	(1150)	s	(319)
	24	δC−H oop	FA	1069	(1089)	w	(25)
	25	δO−H oop	Tfa	942	(1025)	m	(61)
	26	δO−H oop	FA	871	(958)	m	(49)
	27	C═O oop	Tfa	*g*	(782)		(9)
	28	δC−F oop	Tfa	522	(506)	w	(3)
	29	O−C═O oop	Tfa		(267)		(0.01)
	30	Os oop	inter		(224)		(6)
	31	Os twist	inter		(83)		(1)
	32	bend	inter		(55)		(0.2)
	33	CF_3 twist	Tfa		(20)		(0.01)

[a] B3LYP/aug-cc-pVDZ. [b] s, strong; m, medium; w, weak. [c] OH str overlap in the range of 2400−3500 cm^{-1}. [d] ν_{12} and ν_{23} are assumed to lie under the peak at 1188 cm^{-1}. [e] Identified in the far-IR spectrum of FA−Tfa mixtures.[33] [f] Calculated from microwave spectra.[32] [g] Not observed, possibly overlapping with ν_{13}.

TABLE 2: Experimental Hydrogen-Bond-Related Vibrational Frequencies for the FA−Tfa Bimolecule, and FA and Tfa Monomers and Dimers[a]

	FA−Tfa bimolecule		FA		Tfa	
no.	assignment	freq	dimer	monomer	dimer	monomer
4	Tfa C═O	1774			1792 (B_u) 1770 (A_g)[b]	1830
5	FA C═O	1701	1742 (B_u) 1670 (A_g)[c]	1777		
7	FA HOC ip	1403	1450 (B_u)	1223		
9	Tfa HOC ip	1325			1301 (B_u)	1250
25	Tfa δO−H oop	942			908 (A_u)[d]	577[e]
26	FA δO−H oop	871	917 (A_u)[f] 889 (B_g)[g]	642		

[a] All frequencies are in cm^{-1} in this study unless otherwise indicated. All IR vibrational frequencies are compared in the Supporting Information. [b] Liquid-phase Raman spectrum.[2] [c] Gas-phase Raman spectrum.[11] [d] Kagarise reported 903 cm^{-1},[3] Redington and Lin reported 923 cm^{-1} in an Ar matrix.[48] There is no value reported in the literature for the B_g δO−H oop vibration of the Tfa dimer. [e] Identified in the Ne matrix spectrum of Tfa dimer.[48] [f] Values of 917 and 908 cm^{-1} have also been reported.[4,7] [g] Raman-active oop OH.[11]

hydrogen bond than in the Tfa dimer. Now in the FA dimer, the oop δCOH band is 275 cm^{-1} higher than the analogous band in the monomer, again due to the hydrogen-bonding effect. However, that vibration in the bimolecule (ν_{26}) is 18 cm^{-1} *lower* than the analogous vibration (B_g symmetry, Raman active) of the FA dimer. In ν_{26} of the bimolecule, the H atoms move in opposite directions, so the comparison is made with the B_g vibration of the FA dimer. These results indicate that (i) the Tfa−OH is more strongly bound in the bimolecule than in the Tfa dimer, (ii) the FA OH is more weakly bound in the bimolecule than in the FA dimer, and (iii) the increase in hydrogen bond stiffness on the Tfa side is greater than the decrease in hydrogen bond stiffness on the FA side. These different frequency shifts are consistent with the calculated hydrogen bond distances in the bimolecule discussed below.

In-plane HOC bending is also stiffened by dimer formation. In the Tfa dimer, this band is 51 cm^{-1} higher than in monomeric Tfa, and the FA−Tfa band is 24 cm^{-1} higher than in the dimer (Table 2). In the FA dimer, the HOC bending mode is 227 cm^{-1} higher than in monomeric FA, but the FA−Tfa band is 47 cm^{-1} *lower* than in the dimer. These results are also consistent with substantial tightening of the H-bond on the Tfa side of the bimolecule and loosening on the FA side relative to homodimers.

The carbonyl stretching frequencies of the FA−Tfa bimolecule are influenced both by hydrogen bonds donated by the opposite acids, and by strong coupling interactions between the carbonyl groups. Hydrogen bonding weakens the carbonyl bond, often leading to lower carbonyl stretching frequencies.[41] For example, in the Tfa dimer the carbonyl stretch is 38 cm^{-1} lower than in the monomer in the infrared and 60 cm^{-1} lower in the Raman (Table 2).[2] These bands are due respectively to the carbonyl bonds stretching in-phase (B_u) and out-of-phase (A_g). In the FA−Tfa bimolecule, the carbonyl vibrations also occur in in-phase and out-of-phase modes, however, the stretching amplitudes are unequal: the minor, or "driven", bond stretches about one-third the amplitude of the major, or "driving" bond. In ν_4 of the bimolecule, the major amplitude Tfa carbonyl stretch is out-of-phase with the FA carbonyl and is 8 cm^{-1} lower in frequency than the analogous vibration in the Tfa dimer. In the FA dimer, the carbonyl stretch is 35 cm^{-1} lower than that of the monomer in the infrared and is 107 cm^{-1} lower in the Raman. In ν_5 of the bimolecule, the major amplitude FA carbonyl stretch is in-phase with the Tfa carbonyl, and ν_5 is 31 cm^{-1} *higher* than the FA dimer in-phase vibration.

Thus it appears that in the FA−Tfa bimolecule, the carbonyl stretching frequencies are most influenced by the motion of the opposite carbonyl: the high-frequency Tfa carbonyl pulls up the FA carbonyl stretch, and the low-frequency FA carbonyl pulls down the Tfa carbonyl stretch. It is necessary to invoke this argument because, as shown below, the Tfa carbonyl is predicted at a high level of theory to be the same length in the bimolecule as in the Tfa dimer, and the FA carbonyl bond is predicted to be longer in the bimolecule than in the FA dimer.

A low-resolution far-IR spectrum of the FA−Tfa bimolecule was obtained by Clague and Novak.[33] They identified two unique peaks, one at 200 cm^{-1} and one at 112 cm^{-1}. The first was identified as a hydrogen bond stretching vibration of A′ symmetry, which was shifted to 193 cm^{-1} in the spectrum of the perdeuterated acids. The closest predicted vibration in the B3LYP/aug-cc-pVDZ frequency calculation is ν_{20} at 218 cm^{-1}, which rocks the FA molecule in-plane and stretches the two H-bonds alternately. The 200 cm^{-1} peak may also contain the nearby A″ O oop vibration (ν_{30}) whose B3LYP/aug-cc-pVDZ frequency is 224 cm^{-1}. This vibration is likely to be observable, since it has the largest calculated intensity of all the peaks in the far-IR region. The second peak reported by Clague and Novak, which shifts to lower frequency by 4 cm^{-1} on deuteration,[33] is likely to be ν_{22} at a calculated frequency of 120 cm^{-1},

TABLE 3: Calculated and Literature Experimental Parameters of the Formic Acid−Trifluoroacetic Acid Bimolecule[a]

	model chemistry				
parameter	HF/ 6-31++G(d,p)	MP2/ 6-31++G(d,p)	B3LYP/ aug-cc-pVDZ	B3LYP/ aug-cc-pVTZ	exptl
intermolecular distances and angles					
formic H···O Tfa (Å)	1.917	1.774	1.706	1.709	
Tfa H···O formic (Å)	1.793	1.659	1.608	1.611	
formic O···O═C Tfa (Å)	2.865	2.763	2.704	2.704	2.729 ± 0.003[b] 2.69 ± 0.02[c]
Tfa O···O═C formic (Å)	2.753	2.661	2.620	2.621	2.700 ±0.014[b] 2.69 ± 0.02[c]
formic O−H···O	169.7	175.6	176.9	176.3	
Tfa O−H···O	172.3	178.1	179.2	178.6	
FA distances and angles					
O−H (Å)	0.959	0.990	0.999	0.996	
C−H (Å)	1.083	1.090	1.101	1.094	1.077 ± 0.001[b]
C═O (Å)	1.198	1.232	1.226	1.219	1.197 ± 0.008[b]
C−O (Å)	1.300	1.324	1.315	1.310	1.339 ± 0.007[b]
C−O−H	111.6	109.8	110.6	110.9	109.6 ± 0.002[b]
H−C═O	122.5	122.1	121.7	121.8	125.0 ± 0.004[b]
H−C−O	111.9	111.6	112.0	111.9	109.4 ± 0.002[b]
O−C═O	125.6	126.2	126.2	126.3	126.7 ± 0.004[b]
Tfa distances					
O−H (Å)	0.966	1.003	1.012	1.010	
C═O (Å)	1.190	1.228	1.220	1.213	
rotational constants ($B + C$) (GHz)	1.11404	1.13305	1.14715	1.15022	1.15348[b] 1.1545[c]
dipole moment (D)	2.4655	2.7362	2.3982	2.3403	
charge transfer	0.0150	0.0221	0.0323	0.0504	
complexation energy (kcal/mol)[d]					
ΔE	−10.4	−10.7	−13.2		
ΔH (298 K)	−11.7	−11.9	−14.2		−15.8 ± 1.5[c]
ΔG (298 K)	−0.67	−0.72	−2.53		

[a] Complete results for 21 model chemistries are in the Supporting Information. [b] Martinache et al.[32] [c] Costain & Srivastava.[29] [d] Energies were corrected for BSSE using the counterpoise method; ZPVEs for the HF and MP2 methods were scaled by 0.92 and 0.97, respectively, as described by Scott and Radom.[49]

which rocks the Tfa molecule in plane. Martinache et al.[32] also found evidence for an absorption at 146 ± 6 cm^{-1}, which likely corresponds to the calculated A′ vibration at 158 cm^{-1}.

Geometry. Calculated bond distances, nonbonding distances, and bond angles of the FA−Tfa bimolecule are shown in Table 3. Results also include a geometry optimization carried out at the B3LYP/aug-cc-pVTZ level of theory (527 basis functions). The optimum equilibrium geometry has C_s symmetry with one C−F bond eclipsing the Tfa carbonyl, as observed with the Tfa monomer[42] and Tfa dimer.[24] Other conformations of the CF_3 group led to negative frequencies for CF_3 rotation. Proceeding from lower to higher levels of theory, the geometric parameters of the optimized complex tended toward a stronger interaction between monomers, with shorter intermolecular distances (Figure 3) and longer O−H and C═O bonds. Within each computational method, the calculated parameters generally reached asymptotic values as the size of the basis set increased. All model chemistries predicted asymmetric hydrogen bonding within the FA−Tfa complex. At the highest level of theory, the nonbonding O···O and O···H distances were 0.083 Å and 0.098 Å shorter, respectively, on the Tfa H-bond side. The intermolecular O−H−O bond angle was also straighter by 2.5° on the Tfa H-bond side, although that value remained just shy of 180°.

The calculated geometry of the FA−Tfa complex differs in several respects from the one derived from microwave spectra of FA−Tfa complexes containing various isotopically substituted formic acids (Table 3).[32] The two approaches differ mainly in estimates of the intermolecular O···O distances: these were calculated from the microwave spectra to be 2.729 Å for the FA H-bond and 2.700 Å for the Tfa H-bond.[32] The present theoretical calculations suggest that the O···O distances are shorter and more unequal (Figure 3). Other noticeable discrepancies between the microwave-derived geometry and the B3LYP/aug-cc-pVTZ geometry are the C−H bond distance, which is 0.017 Å shorter in the microwave-derived data, and the FA H−O−C bond angle, which is 2.5° smaller. Martinache et al. could not obtain reliable O−H distances, so the authors assumed a value of 0.970 Å for both distances, a number intermediate between the published values for the two monomers.

A useful test of the predicted geometry of a cyclic carboxylic acid dimer in the gas phase is to compare microwave-derived rotational constants with the rotational constants resulting from ab initio or DFT geometry optimization.[9,43] For an asymmetric top such as the FA−Tfa bimolecule, the three rotational constants *A*, *B*, and *C* equal the inherent rotation constants of the complex about axes *a*, *b*, and *c* (Figure 4). The transverse rotations *B* and *C* are of particular interest since they depend on the monomer−monomer separation distance. The sum $B + C$ was obtained from lower resolution microwave spectra by Costain and Srivastava.[29] Although the high-resolution spectra of Martinache et al. yielded values for all three constants,[32] the sum $B + C$ is included in Table 3 and Figure 3 to allow comparison with the earlier data. As shown in Figure 3, the ab initio and DFT-calculated $B + C$ values for FA−Tfa are consistently too low, but at the highest levels of theory used they approach the experimental values.

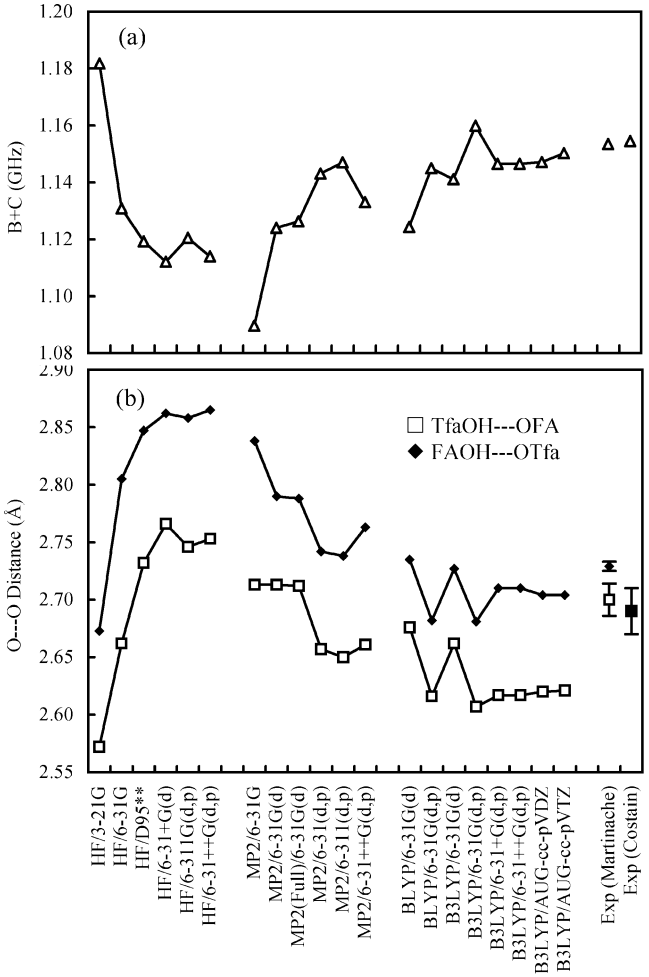

Figure 3. FA−Tfa bimolecule geometric parameters calculated by different model chemistries compared to geometric parameters derived from microwave spectra by Costain and Srivastava[29] and Martinache et al.[32] (a) Rotational constants $B + C$. (b) O···O separation.

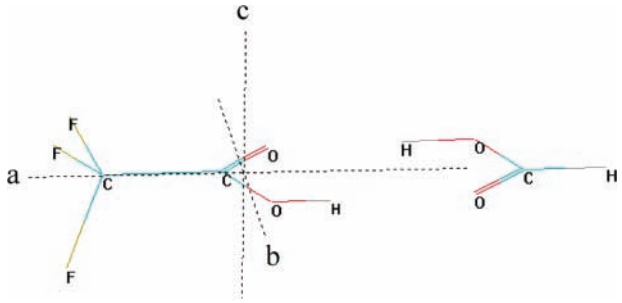

Figure 4. Rotational axes *a*, *b*, and *c* corresponding to the rotational constants *A*, *B*, and *C* of the formic acid−trifluoroacetic acid bimolecule.

In the crystal, the acetic acid−Tfa bimolecule contains intermolecular distances that differ even more than those calculated for FA−Tfa.[38] These are 2.761 ± 0.005 Å on the acetic acid OH side, and 2.571 ± 0.004 Å on the Tfa OH side, compared to the analogous FA−Tfa distances of 2.704 Å and 2.620 Å. The greater difference in the acetic acid−Tfa O···O distances is consistent with the stronger hydrogen bond interactions in this complex compared to FA−Tfa.[29]

Comparing Calculated O−H···O Geometries of the Bimolecule, Dimers, and Monomers. Ab initio and DFT calculations show that in some ways, such as in the geometry of the C−H and CF_3 groups, the FA−Tfa bimolecule closely resembles the FA and Tfa dimers. However, the geometry at the monomer−monomer interface is perturbed significantly compared to the dimers. Table 4 shows the geometric parameters of the H-bonded region of the FA−Tfa bimolecule calculated at the B3LYP/aug-cc-pVDZ level of theory and, for comparison, the analogous distances in FA and Tfa monomers and dimers. For FA and FA dimer, the hybrid DFT geometries in Table 4 agree closely with those obtained by others at this level of theory.[25,27] The present study reports the first hybrid DFT geometries for Tfa and Tfa dimer. These are similar to the values obtained at the MP2/6-31+G(d) level,[24,42] however, the hybrid DFT method predicts closer monomer−monomer contacts. The main differences are in the dimer O···H distance (5.7% less), the dimer O···O distance (3.4% less), and the monomer O−H distance (1% less). All other bond distances differ by 0.5% or less in the two methods.

TABLE 4: Comparison of the B3LYP/AUG-cc-pVDZ Hydrogen-Bond Geometry of the FA−Tfa Bimolecule with FA, FA Dimer, Tfa, and Tfa Dimer[a]

	Tfa	Tfa dimer	FA−Tfa	FA dimer	FA
		Distances (Å)			
Tfa (C═O)···O[b]			2.704	2.667	
Tfa (C═)O···H[b]			1.706	1.665	
FA C═O			1.226	1.218	1.205
FA C−O			1.315	1.310	1.349
FA OH			0.999	1.002	0.973
FA (C═)O···O[c]		2.663	2.620		
FA (C═)O···H[c]		1.660	1.608		
Tfa C═O	1.194	1.220	1.220		
Tfa C−O	1.337	1.308	1.306		
Tfa OH	0.970	1.004	1.012		
		Angles			
Tfa (C═)O···H−O[b]			176.9	178.4	
FA C−O−H			110.6	110.9	107.5
FA (C═)O···H−O[c]		177.3	179.2		
Tfa C−O−H	108.2	110.4	110.5		

[a] See the Supporting Information for comparisons of all geometric parameters. [b] Hydrogen bond donated by formic acid. [c] Hydrogen bond donated by trifluoroacetic acid.

The FA and Tfa O−H distances of the FA−Tfa bimolecule were both assumed to be 0.970 Å in the microwave study by Martinache et al.[32] The B3LYP/aug-cc-pVDZ results estimate that the monomer O−H distances are within 0.003 Å of this value (Table 4), and in the dimers the O−H distances are 0.030 Å longer as a consequence of H-bond formation. In the bimolecule, however, the FA O−H distance is shorter than in the FA dimer by 0.003 Å and the Tfa O−H is longer than in the Tfa dimer by 0.008 Å.

In the case of the intermolecular distances, the calculated distances in the FA and Tfa homodimers are within 0.004 Å of each other, but in the bimolecule the O's on the Tfa−OH side are 0.043 Å closer than in the Tfa dimer, and the O's on the FA−OH side are 0.037 Å farther apart than in the FA dimer. The H-bond O···H distances follow a similar trend: 0.052 Å closer on the Tfa−OH side and 0.041 Å farther apart on the FA−OH side. These subtle geometry changes—3.2% shorter Tfa-donated H-bond length and 2.5% longer FA-donated H-bond compared to the H-bond lengths in the homodimers—indicate that, compared to the dimers, the H-bond donated by FA in the bimolecule is weaker, while that donated by Tfa is stronger. The magnitude of these differences suggest that, relative to the homodimers, the Tfa H-bond is strengthened more in the bimolecule than the FA H-bond is weakened. This would predict a net stabilizing effect on the bimolecule relative to the homodimers, which is indeed observed experimentally and theoretically.

Complexation Energy. Experimentally it has been shown that the FA−Tfa bimolecule is more stable than the FA dimer,

TABLE 5: Complexation Enthalpies for the FA−Tfa Bimolecule, Tfa Dimer, and FA Dimer (Gas-Phase, 298 K)

complex	ΔH (kcal/mol)	method
	Experimental	
$(Tfa)_2$	-14.2 ± 0.2	photoacoustic[a]
	-13.66 ± 2.0	thermal conductivity[b]
	−14.0	infrared[c]
	−14.0	vapor density[d]
	-14.5 ± 0.6	vapor phase NMR[e]
$(FA)_2$	-14.5 ± 0.5	various[f]
FA−Tfa	-15.8 ± 1.5	microwave[g]
	Theoretical[h]	
$(Tfa)_2$	−13.6	B3LYP/6-31G(d)
	−13.0	B3LYP/aug-cc-pVDZ
$(FA)_2$	−11.1	MP2/6-31+G(d)[f]
	−13.7	B3LYP/6-31G(d)[f]
	−13.7	B3LYP/aug-cc-pVDZ
FA−Tfa	−12.1	MP2/6-31+G(d)
	−14.5	B3LYP/6-31G(d)
	−14.2	B3LYP/aug-cc-pVDZ

[a] Sauren et al.[50] [b] Frurip et al.[19] [c] Christian et al.[18] [d] Taylor and Templeman.[51] [e] Lumbroso-Bader et al.[13] [f] Reviewed by Colominas et al.[25] [g] Costain and Srivastava[29] [h] This study unless otherwise referenced. Energies include ZPE and counterpoise BSSE corrections.

which in turn is more stable than Tfa dimer (Table 5). Formation of bimolecules in mixtures of acetic and formic acids with halogenated acids is favored over formation of symmetric dimers due to the lower symmetry number of the bimolecule[34] and stronger monomer−monomer hydrogen bonding.[36] Predicted values for binding energy, enthalpy, and Gibbs free energy for the FA−Tfa bimolecule, calculated at three levels of theory, are shown in Table 3. The calculated enthalpy values are more negative at higher levels of theory. However, the best value obtained in this work (B3LYP/aug-cc-pVDZ) is still 1.5 kcal/mol less than the experimental value (-15.8 ± 1.5 kcal/mol), which was derived from the temperature dependence of the microwave spectrum.[29]

Enthalpies of complexation of FA, Tfa, and the FA−Tfa bimolecule are compared in Table 5. These studies have shown that the FA−Tfa bimolecule is about 1.3 kcal/mol more stable than the FA dimer, and the FA dimer is slightly more stable, by about 0.3 kcal/mol, than the Tfa dimer. The same order is predicted at different levels of theory.

Population Analysis. Mulliken population analysis shows that charge transfer occurs between FA and Tfa in the bimolecule, with FA carrying from 0.015 to 0.050 excess positive charge, depending on the level of theory (Table 3). The calculated dipole moment is 2.340 D at the B3LYP/aug-cc-pVTZ level of theory (Table 3). This is somewhat larger than the dipole moment for Tfa, for which the experimental value is 2.28 D;[44] the value calculated at the same level of theory is 2.249 D. No experimental dipole measurement has been reported for the FA−Tfa bimolecule, however, the dipole moment of the acetic acid−Tfa bimolecule is reported to be 2.99 ± 0.5 D.[31]

Although the FA−Tfa bimolecule is quite polar, this does not necessarily result in more polar OH bonds or in significantly increased partial charges on the bridging hydrogens. The Tfa hydrogen does carry slightly more positive charge than the FA hydrogen in the bimolecule (Figure 5); however, this is also true in the monomers and homodimers. A priori, it would seem that if the Tfa-donated hydrogen bond is stronger and the TfaO−H bond is lengthened in the bimolecule, then the Tfa hydrogen should be more positive relative to that atom in the Tfa dimer. Likewise, if the FA-donated hydrogen bond is weaker

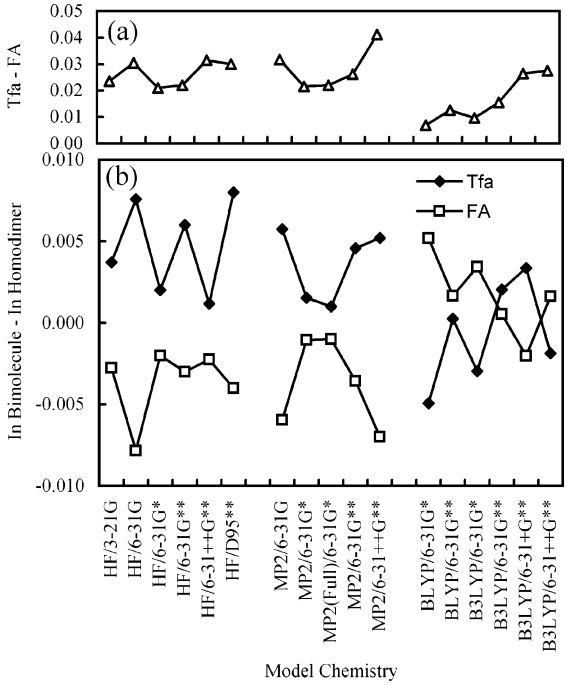

Figure 5. Mulliken population analysis of the charge density on the bridging hydrogens for different model chemistries. (a) In the FA−Tfa bimolecule, the difference between the partial charge on Tfa and FA OH hydrogens. (b) The difference between the partial charge on the acidic hydrogen in the bimolecule and in the homodimer.

relative to the FA dimer, and the FAO−H bond is shortened, then the FA OH hydrogen should be less positive. This notion is supported by calculations carried out at lower levels of theory (Figure 5b) but is contradicted at higher levels of theory, which show that there is essentially no difference in the charge density of a bridging hydrogen in the bimolecule relative to the homodimer. This result points to greater covalent bonding between the monomers of the bimolecule as a source of its enhanced stabilization.

Conclusions

These results provide a partial explanation for the increased stability of carboxylic acid bimolecules containing acids of significantly different acidities, compared to their related homodimers. Most directly affected by complex formation, and clearly displayed in the FT-IR spectrum, are the out-of-plane vibrations of the OH groups that connect the two molecules. Compared with the homodimer, the hydrogen bond donated by Tfa in the bimolecule is tightened considerably judging from the increase in frequency of the out-of-plane vibration. On the other hand, the hydrogen bond donated by FA is loosened in the bimolecule relative to the FA dimer, but the frequency difference relative to the homodimer is only half that seen on the Tfa side. The energy difference equivalent to these frequency differences is less than 0.1 kcal/mol, however, the same relative effects could be expected for the higher energy OH stretching modes. Taken together, these energy differences may be enough to account for the 1.3 kcal/mol stability difference between the bimolecule complex and the FA dimer.

The theoretical calculations reported here still underestimate the complexation enthalpy of the FA−Tfa bimolecule by 1.5 kcal/mol compared to the experimental value, and they overestimate the frequency of the out-of-plane vibrations that are diagnostic of hydrogen bonding within the complex. It is not clear that using ever larger basis sets for these calculations would

improve these predictions, since the trends of vibrational frequency, geometric parameters, and energies versus level of theory appear to change little at the highest levels of theory.

Experimental Section

FT-IR Samples. Reagent-grade trifluoroacetic acid and formic acid (Aldrich) were distilled at atmospheric pressure. Formic acid was initially dehydrated by refluxing over phthalic anhydride.[45] Samples were prepared using a 0.5-L flask connected by a stopcock to a 5-mL sidearm flask. The sidearm was filled with argon, and 5−20 μL of acid was added by syringe through a vacuum-tight septum. The liquid was evaporated into the evacuated large flask, and the total pressure was brought to 1 atm with Ar. Finally, the Ar−acid vapor mixture was admitted into an evacuated 25 mm × 100 mm Spectra-Tech demountable gas cell equipped with NaCl windows, and additional Ar was admitted to make up the pressure to 1 atm.

IR Spectra and Data Analysis. FT-IR spectra were obtained with a Nicolet Magna-560 spectrometer (400−4000 cm^{-1}, 256 scans, 0.5-cm^{-1} resolution, mirror velocity 0.6329 cm/s). In processing interferograms, Happ−Genzel apodization and Mertz phase correction functions, with no zero-filling, were used. Digitized spectra (14 936 points) were analyzed with MS Excel 2002. The residual spectrum, obtained after subtracting scaled monomer and dimer spectra from the total spectrum, was smoothed with Origin software version 7.0 using a 6-point Fourier smoothing function. The 1120−1280 cm^{-1} region was fitted using least-squares analysis (Excel Solver) to a Lorentzian−Gaussian function (eq 1), where A_i is the absorbance at frequency ω_i; and p_j, h_j, and w_j are the fitted values of position, height, and width of each of three peaks; and m is the fraction Lorentzian function. In Figure 1 the derived value of m was 0.432.

$$A_i = \sum_j \left[(1-m) h_j \, e^{-2.772589((\omega_i - p_j)/w_j)2} + \frac{m h_j}{1 + 4((\omega_i - p_j)/w_j)^2} \right] \quad (1)$$

Theoretical Calculations. Calculations were carried out with Gaussian 98 revision A.7 using standard basis sets and default settings.[46] The starting symmetry of the Tfa and FA monomers and FA−Tfa bimolecule was C_s, and for Tfa and FA dimers it was C_{2h}. Results were visualized using the Molekel program.[47] All frequency calculations were carried out using the same method and basis set used for geometry optimization.

Acknowledgment. This work was supported in part by a Grant from the University of Alaska Foundation. Computer time was provided by the Arctic Region Supercomputing Center. Eric Guglielmo carried out preliminary ab initio calculations at the Arctic Region Supercomputing Center. Helpful comments and discussions were provided by L. Claron Hoskins, William Simpson, and Rafail Khairoutdinov.

Supporting Information Available: Geometry parameters of the FA−Tfa bimolecule; (2) thermodynamic parameters of the FA−Tfa bimolecule; (3) comparison of geometric parameters (B3LYP/AUG-cc-pVDZ) for formic acid (FA), FA dimer, trifluoroacetic acid (Tfa), Tfa dimer, and the FA−Tfa bimolecule; (4) comparison of all infrared vibrational frequencies (cm^{-1}) for the gas-phase FA−Tfa acid bimolecule, FA and Tfa monomers and dimers; (5) mulliken population analysis of the FA−Tfa bimolecule. This material is available free of charge via the Internet at http://pubs.acs.org.

References and Notes

(1) Pauling, L.; Brockway, L. O. *Proc. Natl. Acad. Sci. U.S.A* **1934**, *20*, 336−340.
(2) Fuson, N.; Josien, M. L.; Jones, E. A.; Lawson, J. R. *J. Chem. Phys.* **1952**, *20*, 1627−1634.
(3) Kagarise, R. E. *J. Chem. Phys.* **1957**, *27*, 519−522.
(4) Millikan, R. C.; Pitzer, K. S. *J. Am. Chem. Soc.* **1958**, *80*, 3515−3521.
(5) Faniran, J. A.; Patel, K. S.; Nelson, L. O. *J. Phys. Chem.* **1978**, *82*, 1018−1021.
(6) Henderson, G. *J. Chem. Educ.* **1987**, *64*, 88−90.
(7) Marechal, Y. *J. Chem. Phys.* **1987**, *87*, 6344−6353.
(8) Qian, W.; Krimm, S. *J. Phys. Chem. A* **2002**, *106*, 6628−6636.
(9) Madeja, F.; Havenith, M. *J. Chem. Phys.* **2002**, *117*, 7162−7168.
(10) Bertie, J. E.; Michaelian, K. H. *J. Chem. Phys.* **1982**, *77*, 5267−5271.
(11) Bertie, J. E.; Michaelian, K. H. *J. Chem. Phys.* **1982**, *76*, 886−894.
(12) Bertie, J. E.; Michaelian, K. H.; Eysel, H. H.; Hager, D. *J. Chem. Phys.* **1986**, *85*, 4779−4789.
(13) Lumbroso-Bader, N.; Coupry, C.; Baron, D.; Clague, D. H.; Govil, G. *J. Magn. Reson.* **1975**, *17*, 386−392.
(14) Lazaar, K. I.; Bauer, S. H. *J. Am. Chem. Soc.* **1985**, *107*, 3769−3772.
(15) Ito, F.; Nakanaga, T. *Chem. Phys.* **2002**, *277*, 163−169.
(16) Lundin, R. E.; Harris, F. E.; Nash, L. K. *J. Am. Chem. Soc.* **1952**, *74*, 4654−4656.
(17) Almenningen, A.; Bastiansen, O.; Motzfeldt, T. *Acta Chem. Scand.* **1969**, *23*, 2848−2864.
(18) Christian, S. D.; Stevens, T. L. *J. Phys. Chem.* **1972**, *76*, 2039−2044.
(19) Frurip, D. J.; Curtiss, L. A.; Blander, M. *J. Am. Chem. Soc.* **1980**, *102*, 2610−2616.
(20) Jurema, M. W.; Shields, G. C. *J. Comput. Chem.* **1993**, *14*, 89−104.
(21) Bures, M.; Bezus, J. *Collect. Czech. Chem. Commun.* **1994**, *59*, 1251−1260.
(22) Chang, Y. T.; Yamaguchi, Y.; Miller, W. H.; Schaefer, H. F., III. *J. Am. Chem. Soc.* **1987**, *109*, 7245−7253.
(23) Turi, L.; Dannenberg, J. J. *J. Phys. Chem.* **1993**, *97*, 12197−12204.
(24) Szasz, G.; Borisenko, K. B.; Hargittai, I. *THEOCHEM* **1997**, *393*, 111−119.
(25) Colominas, C.; Teixido, J.; Cemeli, J.; Luque, F. J.; Orozco, M. *J. Phys. Chem. B* **1998**, *102*, 2269−2276.
(26) Chojnacki, H.; Andzelm, J.; Nguyen, D. T.; Sokalski, W. A. *Comput. Chem.* **1995**, *19*, 181−187.
(27) Jursic, B. S. *THEOCHEM* **1997**, *417*, 89−94.
(28) Loerting, T.; Liedl, K. R. *J. Am. Chem. Soc.* **1998**, *120*, 12595−12600.
(29) Costain, C. C.; Srivastava, G. P. *J. Chem. Phys.* **1964**, *41*, 1620−1627.
(30) Gautam, H. O. *Indian J. Pure Appl. Phys.* **1970**, *8*, 713−715.
(31) Bellott, E. M.; Wilson, E. B. *Tetrahedron* **1975**, *31*, 2896−2898.
(32) Martinache, L.; Kresa, W.; Wegener, M.; Vonmont, U.; Bauder, A. *Chem. Phys.* **1990**, *148*, 129−140.
(33) Clague, D.; Novak, A. *J. Mol. Struct.* **1970**, *5*, 149−152.
(34) Affsprung, H. E.; Christian, S. D.; Melnick, A. M. *Spectrochim. Acta* **1964**, *20*, 285−290.
(35) Christian, S. D.; Affsprung, H. E.; Lin, C. *J. Chem. Soc. B* **1965**, 2378−2381.
(36) Kohler, F.; Findenegg, G. H.; Bobik, M. *J. Phys. Chem.* **1974**, *78*, 1709−1714.
(37) Abrman, P.; Malijevska, I. *Fluid Phase Equilib.* **1999**, *166*, 47−52.
(38) Schilling, M.; Bartmann, K.; Mootz, D. *J. Fluorine Chem.* **1995**, *73*, 225−228.
(39) Rode, B. M.; Engelbrecht, A.; Jakubetz, W. *Chem. Phys. Lett.* **1973**, *18*, 285−289.
(40) Curtiss, L. A.; Blander, M. *Chem. Rev.* **1988**, *88*, 827−841.
(41) Scheiner, S. *Hydrogen Bonding A Theoretical Perspective*; Oxford University Press: New York, 1997; p 200.
(42) Antolinez, S.; Alonso, J. L.; Dreizler, H.; Hentrop, E.; Sutter, D. H. *Z. Naturforsch., A: Phys. Sci.* **1999**, *54*, 524−538.
(43) Neuheuser, T.; Hess, B. A.; Reutel, C.; Weber, E. *J. Phys. Chem.* **1994**, *98*, 6459−6467.
(44) McClellan, A. L. *Tables of Experimental Dipole Moments*; W. H. Freeman & Co.: San Francisco, 1963; p 125.
(45) Perrin, D. D.; Armarego, W. L. F., *Purification of Laboratory Chemicals*, 3rd ed.; Pergamon Press: Oxford, 1988; p 185.

(46) Frisch, M. J.; Trucks, G. W.; Schlegel, H. B.; Scuseria, G. E.; Robb, M. A.; Cheeseman, J. R.; Zakrzewski, V. G.; Montgomery, J. A., Jr.; Stratmann, R. E.; Burant, J. C.; Dapprich, S.; Millam, J. M.; Daniels, A. D.; Kudin, K. N.; Strain, M. C.; Farkas, O.; Tomasi, J.; Barone, V.; Cossi, M.; Cammi, R.; Mennucci, B.; Pomelli, C.; Adamo, C.; Clifford, S.; Ochterski, J.; Petersson, G. A.; Ayala, P. Y.; Cui, Q.; Morokuma, K.; Malick, D. K.; Rabuck, A. D.; Raghavachari, K.; Foresman, J. B.; Cioslowski, J.; Ortiz, J. V.; Stefanov, B. B.; Liu, G.; Liashenko, A.; Piskorz, P.; Komaromi, I.; Gomperts, R.; Martin, R. L.; Fox, D. J.; Keith, T.; Al-Laham, M. A.; Peng, C. Y.; Nanayakkara, A.; Gonzalez, C.; Challacombe, M.; Gill, P. M. W.; Johnson, B. G.; Chen, W.; Wong, M. W.; Andres, J. L.; Head-Gordon, M.; Replogle, E. S.; Pople, J. A. *Gaussian 98*, revision A.7; Gaussian, Inc.: Pittsburgh, PA, 1998.

(47) Portmann, S. *Molekel* 4.3.win32; CSCS/ETH Zurich: Geneva, 2002.

(48) Redington, R. L.; Lin, K. C. *Spectrochim. Acta, Part A* **1971**, *27*, 2445−2460.

(49) Scott, A. P.; Radom, L. *J. Phys. Chem.* **1996**, *100*, 16502−16513.

(50) Sauren, H.; Winkler, A.; Hess, P. *Chem. Phys. Lett.* **1995**, *239*, 313−319.

(51) Taylor, M. D.; Templeman, M. B. *J. Am. Chem. Soc.* **1956**, *78*, 2950−2953.